Structural and dielectric studies in the $(Ba_{0.9}Ca_{0.1})(Ti_{1-x}Sn_x)O_3$ system

KI HYUN YOON, JAE HYUN KIM, KYUNG HWA JO, HYO ILL SONG, SANK OK YOON, CHANG SOO KIM
Department of Ceramic Engineering, Yonsei University, Seoul, Korea

The variation in lattice constant and dielectric constant in the $(Ba_{0.9}Ca_{0.1})(Ti_{1-x}Sn_x)O_3$ system have been investigated for compositions from $x = 0$ to $x = 0.20$. The *a* axis lattice constant increases at room temperature as substitution of tin for titanium increases, while the *c* axis lattice constant decreases. The dielectric constant increases and the Curie temperature is shifted to lower temperature as the amount of tin increases.

1. Introduction

As is well known, barium titanate ceramics have exceedingly high dielectric constants with low dissipation factors and have been widely used as capacitor materials [1, 2]. However, a big disadvantage is the high temperature coefficient of capacitance near the Curie point, due to the phase transition from the tetragonal to the cubic phase. Therefore, ceramic capacitors having the perovskite structure have been usable only in certain limited temperature ranges.

However, these characteristics of perovskite ceramic materials can be improved through the formation of solid solutions by substitution with suitable ions which make the cubic structure more stable relative to the tetragonal structure than in pure $BaTiO_3$. Drexler [3] reported that the Curie temperature of barium titanate could be shifted to other temperatures by formation of solid solutions with other double oxides, for instance alkaline-earth titanates, lead titanate, various stannates and zirconates. Various reports [4–7] have suggested that the temperature coefficient of the dielectric constants can be decreased by the substitutional solid solution of other perovskite materials having similar structures to barium titanate.

In this study, the dependence of dielectric properties on additives has been investigated together with the variation in lattice constant and the microstructure of the sintered materials as Ba^{2+} ions are replaced by Ca^{2+} ions, and Ti^{4+} ions replaced by Sn^{4+} ions over the range of solid solubility of barium titanate ceramics.

2. Experimental details

2.1. Preparation of specimens

$BaCO_3$, $CaCO_3$, TiO_2 and SnO_2 with purities above 99.9% were used as raw materials. The composition of $(Ba_{0.9}Ca_{0.1})(Ti_{1-x}Sn_x)O_3$ used in this study varied from $x = 0$ to $x = 0.20$. Each batch was wet ball-milled for 10 h with ethyl alcohol as mixing agent and dried completely. The mixed powders were calcined for 2.5 h at 1250° C in a platinum crucible and then ball-milled once more. The calcined materials were confirmed as solid solutions by X-ray diffraction analysis, and then isostatically pressed into pellets 14 mm in diameter and 4 mm in thickness under a pressure of 20 000 psi. These were sintered in a platinum crucible at 1430° C for 0.5, 4 and 8 h in an electrical furnace and then cooled slowly. The sintered specimens were ground and polished to the same thickness with SiC paper and cleaned with acetone and distilled water. The relative densities of the specimens were determined by ASTM test method C373–72 (1977). Electrodes were connected to both surfaces of the specimens with silver paste for electrical measurements.

2.2. Measurements

The crystalline structure of the sintered specimens were examined by X-ray diffraction analysis using CuKα radiation. The specimens were polished to assure cleanliness and etched with an H_3PO_4 solution at 80° C for 1 h. A metallurgical microscope (Nikon AFX Type 104, Japan) was used for microstructural observation.

Dielectric properties of the specimens were measured at 1.02 KHz over the temperature range from 130 to −40° C by LCR meter (Ando, AG4303, Japan). The measuring chamber could be cooled with liquid nitrogen or heated by a heating coil.

TABLE I Variation of lattice parameters and densities with SnO_2 content and soaking time for $(Ba_{0.9}Ca_{0.1})(Ti_{1-x}Sn_x)O_3$

Lattice parameters	Mole fraction (x) Soaking time (4 h)			Mole fraction ($x = 0.1$) Soaking time (h)		
	0	0.1	0.2	0.5	4	8
a (nm)	0.3954	0.3998	0.4015	0.3986	0.3998	0.4001
c (nm)	0.4057	0.4008	0.4007	0.4017	0.4008	0.4007
c/a	1.026	1.003	0.998	1.008	1.003	1.002
Relative density (%)	96.6	95.2	94.2	91.5	95.2	94.1

0022–2461/88 $03.00 + .12

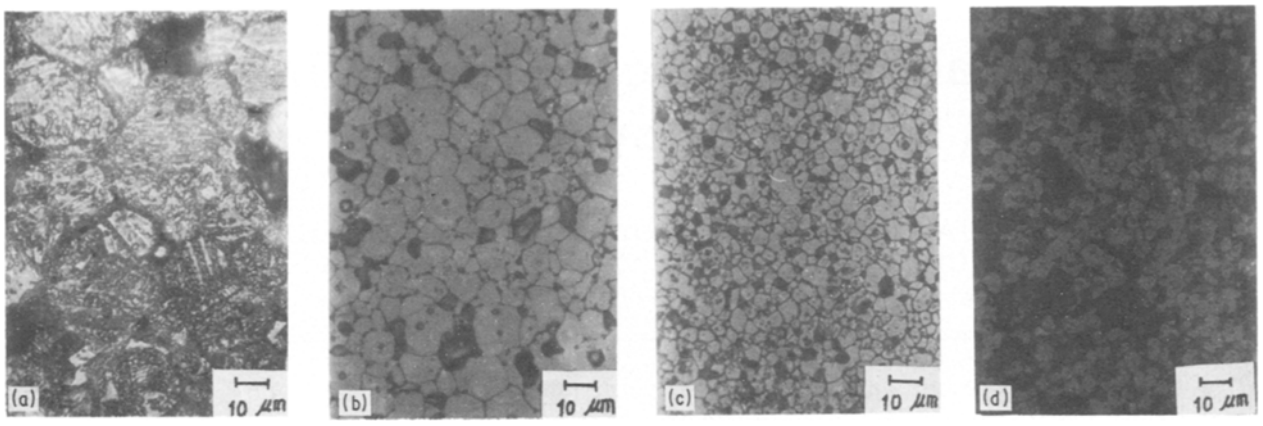

Figure 1 Microstructure of $(Ba_{0.9}Ca_{0.1})(Ti_{1-x}Sn_x)O_3$ sintered at 1430° C for 8 h. (a) $x = 0$, (b) $x = 0.10$, (c) $x = 0.125$, (d) $x = 0.20$.

3. Results and discussion

3.1. Crystalline structure and microstructure

When CaO, SnO_2 and other additives are added to $BaTiO_3$, the difference in ionic radius for the cations prohibits the formation of complete solid solutions over the full range of compositions, and this results in regions of immiscibility between the $BaTiO_3$ and each set of additives [8, 9]. Drust *et al.* [9] reported that $CaTiO_3$ was completely soluble within the range up to about 20 mol % at 1325° C in $BaTiO_3$. With SnO_2, it is possible to form solid solutions with $BaTiO_3$ to above 45 mol % [5]. The compositions used in these experiments formed solid solutions without other second phases and this was confirmed by X-ray diffraction analysis. Table I shows the variations in lattice constants a and c computed from the X-ray diffraction peaks for the $(Ba_{0.9}Ca_{0.1})(Ti_{1-x}Sn_x)O_3$ system sintered at 1430° C as a function of the mole fraction of SnO_2 and the soaking time. Attention was mainly given to the behaviour of the (3 3 2) and (4 2 2) planes as they offered the best basis for reaction studies [8]. Because the value of $\sin\theta$ is higher for larger values of θ, the change for the 2θ value was accurately observed.

As shown in Table I, the specimen with no SnO_2 displays clearly the tetragonal phase with a c/a value of 1.026; this agrees well with McQuarrie's report [6], which describes variation of lattice constants with composition for the barium titanate–calcium titanate binary.

The a axis lattice constant is elongated and the c axis value is shortened as the amount of SnO_2 increases, and the a axis is elongated and the c axis is shortened as the soaking time is lengthened. These variations of the lattice parameters can be explained in terms of the phase transition from the tetragonal to the cubic structure due to adding SnO_2 and the homogeneous distribution of substitutional Sn^{4+} ions due to the thermal treatment.

The microstructures of the specimens sintered at 1430° C for 8 h are presented in Fig. 1, which shows that the grain size decreases and porosity increases as the amount of SnO_2 increases due to its grain growth inhibition behaviour. Also, the densities of the specimens are decreased when tin is substituted for titanium as shown in Table I. While domains can be observed in the grains with no SnO_2 [10], these domains disappear after adding SnO_2. The reason is that the occurrence of 90° twinning is rarely observed in fine grains and it is hard for domains to form. However in coarse grains, the internal stress is minimized through the frequent occurrence of 90° twinning [11].

3.2. Dielectric property

Figs 2–4 shows the variation of dielectric constant with the amount of SnO_2 in the $(Ba_{0.9}Ca_{0.1})(Ti_{1-x}Sn_x)O_3$ system sintered at 1430° C for 0.5, 4 and 8 h, respectively. It can be seen that below the Curie temperature,

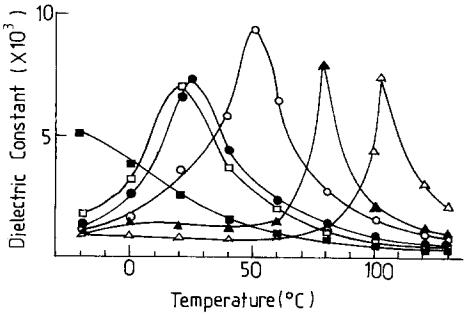

Figure 2 Dielectric constant against temperature for $(Ba_{0.9}Ca_{0.1})(Ti_{1-x}Sn_x)O_3$ sintered at 1430° C for 0.5 h. x = △, 0; ▲, 0.05; ○, 0.10; ●, 0.125; □, 0.15; ■, 0.20.

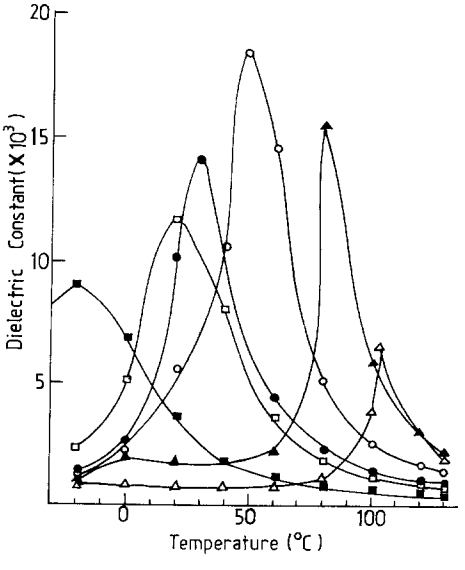

Figure 3 Dielectric constant against temperature for $(Ba_{0.9}Ca_{0.1})(Ti_{1-x}Sn_x)O_3$ sintered at 1430° C for 4 h. x = △, 0; ▲, 0.05; ○, 0.10; ●, 0.125; □, 0.15; ■, 0.20.

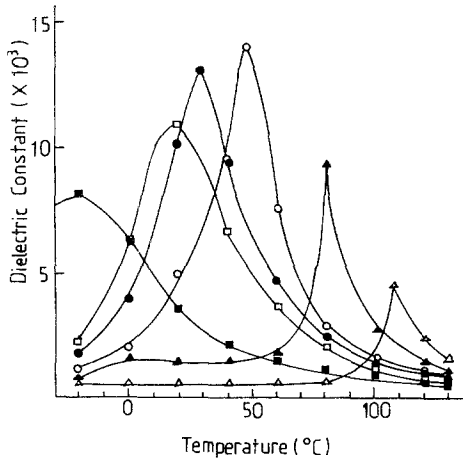

Figure 4 Dielectric constant against temperature for $(Ba_{0.9}Ca_{0.1})(Ti_{1-x}Sn_x)O_3$ sintered at 1430° C for 8 h. x = △, 0; ▲, 0.05; ○, 0.10; ●, 0.125; □, 0.15; ■, 0.20.

the dielectric constants increase with increasing amount of SnO_2 and the Curie temperatures shift to lower temperatures. In the $BaTiO_3$ structure, the Ba^{2+} (0.134 nm in ionic radius) is replaced by smaller Ca^{2+} (0.099 nm) and Ti^{4+} (0.076 nm) replaced with larger Sn^{4+} (0.093 nm). As a result, the observations can be explained in terms of the decrease in polarizability due to more tightening of the bond between the Sn^{4+} substituted for Ti^{4+} ions and the O^{2-} ions [12]. With an increasing amount of SnO_2, and a corresponding increase in the a axis as shown in Table I, the phase transition from tetragonal to cubic structure makes the Curie temperature shift to a lower temperature.

In these figures, as the grain size decreases, that is, the amount of SnO_2 increases, the dielectric constant increases. This can be explained in terms of internal stress as reported by Buessem [11]. When $BaTiO_3$ is cooled through the Curie temperature, the phase transition from cubic to tetragonal changes the lattice constant. This results in stress at the grain boundaries. Therefore the high dielectric constant in fine grains is explained by the difficulty of 90° twinning, and hence the presence of internal stress below the Curie temperature. If interface domains are formed through 90° twinning so that the polar axes are perpendicular to each other, the internal stress is minimized [13].

As shown in Figs 2–4, when the SnO_2 is more than 10 mol %, the peaks are broadened and do not show a definite transition temperature. This may be explained in terms of the diffuse phase transition [14], which results from spatial composition fluctuation or polarization fluctuation as suggested by Hegenbarth [15] and Smolenskii [16]. Because of the internal field stress accompanied by these fluctuations, the phase transition temperature of each microregion might be different. Therefore, the curves do not present the sharp phase transition temperature.

The value of the dielectric constant rises and falls with increasing soaking time as shown in Figs. 2–4. This can be explained by the difference in average grain size in the microstructure as shown in Fig. 5. When the $BaTiO_3$ ceramic transforms from the cubic paraelectric into the tetragonal ferroelectric phase, the internal stress in the microstructure increases strongly [14]. The grain size thus has an immense influence on the temperature characteristics. Hennings *et al.* [14] reported that by reducing the average grain size of ceramic (Ba, Ca)(Ti, Zr)O_3 from 40 to $\approx 3\,\mu$m, the Curie maximum (dielectric constant) decreased from 16 000 to 3000. Specimen (a) in Fig. 5 has a relatively low dielectric constant and density due to insufficient soaking time.

4. Conclusions

1. With increasing amount of SnO_2 and soaking time in the $(Ba_{0.9}Ca_{0.1})(Ti_{1-x}Sn_x)O_3$ system, the a axis lattice constant is elongated and the c axis value is shortened due to the phase transition from tetragonal to cubic structure.

2. As the amount of SnO_2 increases, the dielectric constant increases below the Curie temperature. As substitution of Sn^{4+} ions for Ti^{4+} ions increases, the Curie temperature corresponding to the phase transition from tetragonal to cubic structure shifts to a lower temperature, and the curves are broadened due to diffuse phase transitions.

References

1. A. L. GRAY and J. M. HERBERT, *ACUSTICA* **6** (1956) 229.
2. R. J. LOCKHART and J. MAGDER, *J. Amer. Ceram. Soc.* **49** (1966) 299.
3. O. DREXLER and B. R. SCHAT, "Science of Ceramics" Vol. 1 (Academic Press, 1961) p. 239.
4. G. H. JONKER and W. KWESTOO, *J. Amer. Ceram. Soc.* **41** (1958) 390.
5. W. W. COFFEEN, *ibid.* **36** (1953) 215.
6. M. MCQUARRIE and F. W. BEHNKE, *ibid.* **37** (1954) 539.
7. D. HENNINGS and H. SCHREINMACHER, *Mater. Res. Bull.* **12** (1977) 1221.
8. R. H. DUNGAN, D. F. KANE and L. R. BICKFORD Jr., *J. Amer. Ceram. Soc.* **35** (1952) 318.
9. G. DRUST, M. GROTENHIUS and A. G. BARKOW, *ibid.* **33** (1950) 133.
10. R. C. DEVRIES and E. BURKE, *ibid.* **40** (1957) 200.

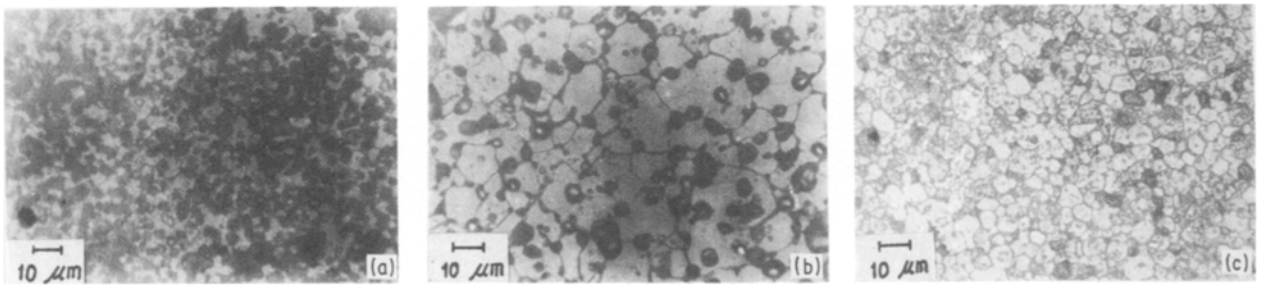

Figure 5 Microstructures of $(Ba_{0.9}Ca_{0.1})(Ti_{0.875}Sn_{0.125})O_3$ sintered at 1430° C for (a) 0.5, (b) 4 and (c) 8 h.

11. W. R. BUESSEM, L. E. CROSS and A. K. GOSWAMI, *ibid.* **49** (1966) 33.
12. J. C. SLATER, *Phys. Rev.* **78** (1950) 748.
13. W. R. COOK Jr., *J. Amer. Ceram. Soc.* **39** (1956) 17.
14. D. HENNINGS, A. SCHNELL and G. SIMON, *ibid.* **65** (1982) 539.
15. E. HEGENBARTH, *Ferroelectrics* **20** (1978) 79.
16. G. A. SMOLENSKII, *J. Phys. Soc. Jpn Suppl.* **28** (1970) 26.

Received 4 September 1986
and accepted 20 March 1987